Effect of Constricted Polymerization Time on Nanofiltration Membrane Characteristic and Performance: A Study Using the Donnan Steric Pore Flow Model

A. L. Ahmad,[1] B. S. Ooi,[1] A. Wahab Mohammad,[2] J. P. Choudhury[1]

[1]*School of Chemical Engineering, Engineering Campus, Universiti Sains Malaysia, Seri Ampangan, 14300 Nibong Tebal, S.P.S, Penang, Malaysia*
[2]*Department of Chemical and Process Engineering, Universiti Kebangsaan Malaysia, 43600, Bangi, Selangor, Malaysia*

Received 16 January 2004; accepted 26 April 2004
DOI 10.1002/app.20904
Published online in Wiley InterScience (www.interscience.wiley.com).

ABSTRACT: Polyamide composite nanofiltration membranes are fabricated under constricted polymerization time. The membranes were characterized for pore size, effective thickness/porosity as well as effective membrane charge density using the Donnan Steric Pore Flow Model. The effect of polymerization (reaction) time on the membrane characteristics and membrane performance (flux and rejection) was studied. The effect of polymerization time on pore size is not significant for reaction times less than 120 s but the effective thickness/porosity seems to be increasing proportionally with polymerization time. Effective membrane charge density for all the membranes depended on the degree of condensation and hydrolysis process. Polymerization time is an important process condition that could change the effective thickness/porosity, pore size, and effective volume charge density and subsequently affect the membrane performance in terms of flux and rejection. © 2004 Wiley Periodicals, Inc. J Appl Polym Sci 94: 394–399, 2004

Key words: membranes; polyamides; composites

INTRODUCTION

Nanofiltration (NF) can be considered to be a relatively new type of pressure-driven membrane compared to reverse osmosis and ultrafiltration. The higher flux and lower operating pressure of nanofiltration promote the feasibility of the membrane in applications involving both water and wastewater treatment processes. Nowadays, nanofiltration has been widely studied for wastewater treatment such as removal of pesticides,[1] arsenic,[2] soil leachate,[3] and dyes.[4] Recently, nanofiltration membranes were also studied for their application in the bioprocess,[5] food,[6] and drinking water industries.[7]

Polyamide (PA) composite membranes have been widely used for NF due to their high permeation performances. Most of them have been generally prepared by forming thin PA active layers on microporous supports. The separation performance of composite nanofiltration membranes prepared by the interfacial polymerization (IP) method depends on several variables, such as concentration of reactant in the aqueous and organic phase, reaction time, temperature, and humidity. Many studies have been carried out on how polymerization time affects membrane performance. A research on the effect of dip time in organic solution shows that different trends of water permeability can be obtained for different reaction times depending on the ratio of *m*-phenylene diamine and *m*-aminophenol.[8] Another study on the structure–performance correlation of polyamide thin film composite membranes has been carried out using Attenuated Total Reflectance Infrared (ATR-IR) spectroscopy. From this study, it was found that the critical parameters for thin film coating were reaction time, relative humidity, and coating temperature. These parameters play an important role in determining the structure of the interfacially polymerized surface film and subsequently the membrane performance.[9] Lu et al.[10] pointed out that the key of the IP method was to select the right partition coefficient of the reactants in the two-phase solution and to set the appropriate diffusion speed of the reactants to achieve the ideal degree of densification of the membrane surface.

Analysis of the membrane characteristic could be carried out using the Donnan Steric Pore Flow Model (DSPM). According to the DSPM, the membranes were assumed to consist of a bundle of identical straight cylindrical pores. The electrolyte transported through the membrane cylindrical pores is controlled by the pore size (r_p), effective thickness/porosity ($\Delta x/A_k$), and the effective membrane charge density (X). By understanding the membrane fabrication conditions, such as reactant concentration and reaction

Correspondence to: A. L. Ahmad (chlatif@eng.usm.my).

time, membranes with specific characteristic (r_p, $\Delta x/A_k$, and X) could be tailor-made.

Up to now several studies have tried to relate the membrane performance to the reaction time and many commercialized membranes have been characterized using the DSPM.[11,12] However only a few studies were carried out to investigate the effect of reaction time on pore size, effective thickness/porosity, and effective membrane charge density. This relationship is very important to study the behavior of flux and rejection in nanofiltration membrane. As suggested by Chen et al.,[13] the preparation condition for different thin film composite nanofiltration membranes still requires further investigation. Therefore, the objective of this paper is to study the effect of reaction time on the membrane characteristics including pore size, effective thickness/porosity, and effective membrane volume charge. These characteristics were related to the membrane performance in terms of flux and rejection.

METHODS

Materials

The polysulfone Udel P-1700 (M_n: 17,000) was a product of Union Carbide Corp. Piperazine (PIP), 3,5-diaminobenzoic acid (BA), *n*-hexane, sodium chloride, and glucose were supplied by Merck Company, Germany. *N*-Methylpyrrolidone (MPD) and trimesoyl chloride (TMC) were purchased from Fluka and polyvinylpyrrolidone was from Sigma-Aldrich Co. The tightly woven polyester, style 0715 Dacron fabric was supplied by Texlon Corp. (USA).

Preparation of polysulfone support layer

The polysulfone support was prepared by dissolving 15% polysulfone (Udel P-1700) in *N*-methylpyrrolidone with 18% polyvinylpyrrolidone as the pore-former. The solution was casted onto a tightly woven polyester fabric with a nominal thickness of 150 μm. The membrane then was immersed into a water bath for at least 24 h until most of the solvent and water soluble polymer was removed.[14]

Fabrication of thin film composite (TFC) membranes

The support layer, which was taped onto a glass plate, was immediately dipped into an aqueous diamine solution containing 2 wt/wt % PIP and 0.1 wt/wt % 3,5- BA for 5 min at ambient temperature. The excess solution from the impregnated membrane surface was removed using a rubber roller. The membrane was then dipped into *n*-hexane solution, which consists of 0.1 wt/vol % TMC. The reaction was carried out at predetermined times of 10, 15, 30, 45, 60, 75, and 120 s.

Hypothetical membrane parameters estimation

To determine the pore size (r_p), effective thickness/porosity ($\Delta x/A_k$), and effective volume charge density (X) of the hypothetical membrane, the DSPM was used.[15,16] The curve fitting for real rejection versus volumetric flux of glucose was carried out using curve-fitting software (Sigma Plot 5.0), which utilizes the Levenberg–Marquardt method. Through the fitted curve, the pore size (r_p) and effective thickness/porosity ($\Delta x/A_k$) were obtained. From the curve fitting for real rejection versus volumetric flux of NaCl the effective charge density was determined.

Membrane permeation test

The membrane permeation test was carried out using the Amicon 8200 stirred cell at five different pressures: 150, 250, 350, 400, and 450 kPa. The membrane was cut to a diameter of 5.5 cm (effective area of 28.27 cm^2) and then mounted at the bottom of the stirred cell. For each operating pressure, fresh solution was used as a feed. Bulk feed concentration was calculated based on the average of initial and final feed concentration. Nitrogen gas was used to pressurize the water flux through a membrane. The solution was stirred at a speed of 350 rpm to reduce concentration polarization. The feed solutions were pure water, 0.01*M* NaCl, and 300 ppm glucose solution. The NaCl permeate concentrations were measured using a conductivity meter (Hanna Instruments, Italy, Model HI8633), while the glucose feed and permeate concentration was analyzed using a colorimetric method based on a treatment with phenol and sulfuric acid.[17] After the solution stood for 30 min, the absorbance at 485 nm was measured using a spectrophotometer (Thermo Spectronic, USA, Model GENESYS 20).

Each membrane was subjected to pressure pretreatment at 500 kPa for 1 h before the permeation experiments. The flux was equilibrated for the passage of the first 20 mL permeate while the following 10 mL permeate was collected for concentration analysis. All the results presented are averaged data obtained through three membrane samples with a variation of $\pm$ 10%.

RESULTS AND DISCUSSION

Effect of polymerization time on pore size (r_p) and effective thickness/porosity ($\Delta x/A_k$)

The effect of polymerization time on r_p and $\Delta x/A_k$ are shown in Figures 1 and 2, respectively. Basically, the membranes produced have a pore size around 0.5 nm. As shown in Figure 1, the average pore size increases slightly for polymerization times between 10 and 75 s (which could be considered constant throughout the reaction time). However, the pore size started to in-

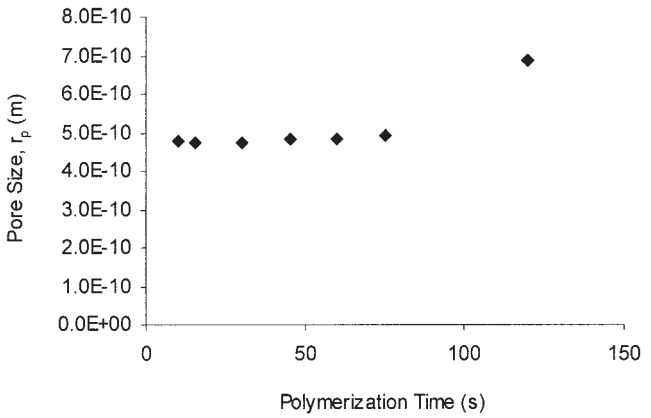

Figure 1 Effect of polymerization time on pore size, r_p.

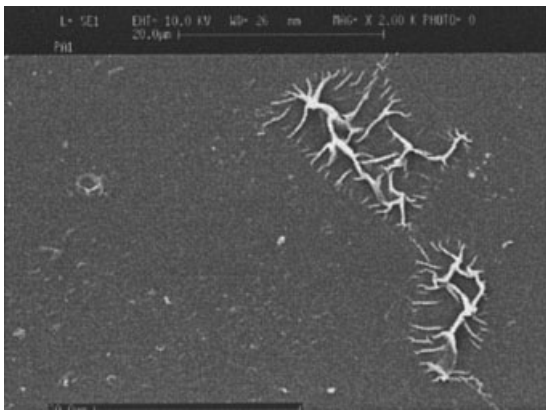

Figure 3 Surface structure of PAt-30.

crease as much as 39% from 75 to 120 s. This is because, at longer reaction times, the adjacent pores coalesced to produce a bigger pore size.

During the polymerization process, the hydrolysis process will compete with the condensation reaction to produce HCl as a side product and a carboxyl group, respectively. Higher content of –COOH groups leads to a higher ratio of hydrophilic groups in the membrane.[18] Consequently, exceeding water uptake produces a loose skin structure. This was why the pore size was larger at higher reaction times.

Contrary to the effect on pore size, the effect of polymerization time on effective thickness/porosity ($\Delta x/A_k$) was more prominent. As shown in Figure 2, $\Delta x/A_k$ increased linearly with an increase in polymerization time. Since $\Delta x/A_k$ was a cumulative term for both effective thickness and porosity, the increase in $\Delta x/A_k$ could be attributed to either the increase in effective thickness or the decrease in porosity. Overall, under polymerization times of 75 s, the membrane produced has quite a similar pore size. Therefore, it was deduced that the increase of $\Delta x/A_k$ was mainly caused by the film growth. Another interesting feature that had been exhibited by the polypiperazinamide membrane was the structure of the skin layer. The membrane surface became rougher at higher reaction times. The surface observed under a scanning electron microscope showed that the rough surface was actually formed by the folded skin layer as shown in Figures 3 and 4 for membranes polymerized at 30 and 60 s, respectively. The folded layer was caused by the extended polymerization process of piperazine and trimesoyl chloride. As illustrated, the folded skin layer for the membrane polymerized under 60 s is widely distributed and thicker than the membrane polymerized at 30 s. This folded layer is thicker and exerts more resistance to the water flow. The growing thickness could be further confirmed by the increase of $\Delta x/A_k$.

If unity porosity was assumed, the rate of film thickness growth after 10 s would be proportional to polymerization time. This information was very important to relate the membrane performance with the polymerization time. For example, to prepare an effective layer of less than 1 μm, the polymerization time should not be more than 10 s.

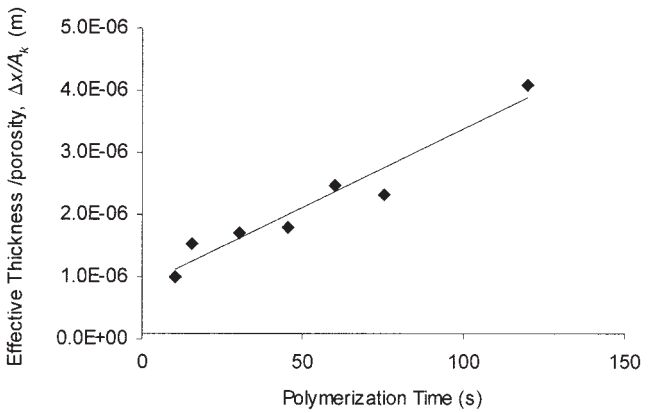

Figure 2 Effect of polymerization time on effective thickness/porosity.

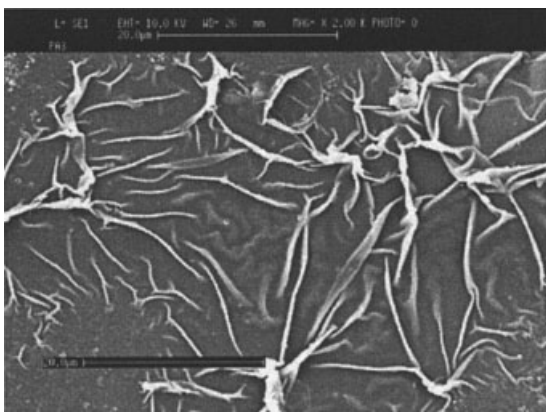

Figure 4 Surface structure of PAt-60.

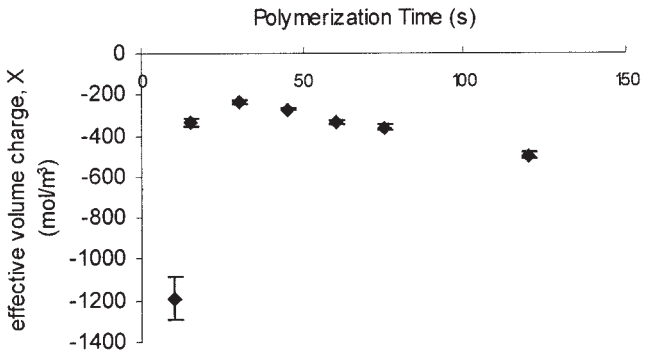

Figure 5 Effect of polymerization time on effective volume charge density.

In contrary to the phenomenon observed by Krantz and Chai[19] in interfacial polymerization between *m*-phenylenediamine (MPD) in water and TMC in hexane, the growth of the IP film thickness becomes self-limiting after 40 s. However, for the reaction in this system with PIP and 3,5-BA in aqueous solution, the film growth was not a limiting factor even at 120 s. This showed that the MPD–TMC polyamide layer was denser compared to the PIP/BA–TMC polyamide layer.

The IP film, which forms the selectively permeable layer, can be made quite thin (< 0.1 μm).[19] However, in this system, to produce a skin layer less than 0.1 μm, which is to be solely controlled by reaction time, seems difficult due to the high film growth rate. Therefore, other parameters such as reactant concentration should be investigated.

Figures 1 and 2 showed that the effect of reaction time on $\Delta x/A_k$ was more significant compared to its effect on r_p. It can be concluded that the time factor was a crucial processing condition to produce an ultrathin *in situ* polymerized skin layer.

Effect of polymerization time on effective volume charge density, *X*

The effect of polymerization time on effective volume charge density was shown in Figure 5. Since the reaction was carried out without the use of any acid acceptor, the HCl produced under this condensation process was not removed instantaneously. The membranes showed that they were negatively charged when characterized using 0.01*M* NaCl. The result agreed well with the finding of other researchers in which polyamide nanofiltration membranes showed negative charges at a neutral pH.[20–22]

There were three mechanisms involved in the film layer formation, namely, film growth, crosslinking, and hydrolysis. Film growth and crosslinking were likely to increase the positive charge of the membrane because of the H^+ produced during the condensation process. On the other hand, hydrolysis was the root for negative charge because of the carboxyl groups ($-COO^-$) introduced. It was suspected that the proton from the condensation process bound itself to the piperazine and converted to $\equiv N{:}H^+$, which was positively charged. During polymerization, the hydrolysis process will compete with the crosslinking process to produce carboxyl groups ($-COO^-$) and $\equiv N{:}H^+$ respectively.

Figure 5 showed that the membrane acquired its highest net negative charge at the polymerization time of 10 s. The charge density was reduced drastically if the reaction was allowed to continue for another 5 s because film growth and crosslinking were likely to take place immediately. As both of these mechanisms produced the proton, the negative charge density was reduced. Starting from 45 s, crosslinking and film growth were slowed down and the mechanism was overtaken by the hydrolysis process. As the hydrolysis process generates more carboxyl groups, the membrane consequently resumes its negative charge. The other explainable reason for higher charge density at longer reaction time was the incorporation of 3,5-diaminobenzoic acid. This is because the reactivity of 3,5-diaminobenzoic acid to trimesoyl chloride was comparatively lower than the piperazine. This phenomenon was well illustrated in Figure 5 where the charge density was reduced five times from –1,190 mol/m^3 at 10 s polymerization time to –273 mol/m^3 at 45 s polymerization time. This indicated that the effect of polymerization time on membrane charge density was really significant.

Effect of reaction time on pure water permeability (PWP)

Figure 6 showed that the value of pure water permeability was reduced as much as 55.5% from 11.09

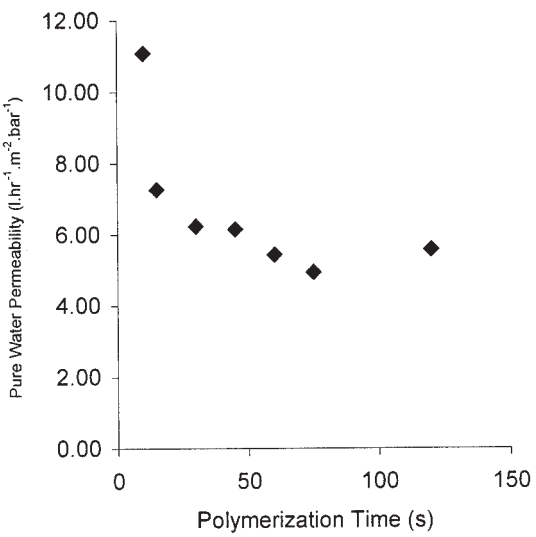

Figure 6 Effect of polymerization time on pure water permeability.

$L \cdot hr^{-1} \cdot m^{-2} \cdot bar^{-1}$ at polymerization time of 10 s to 4.94 $L \cdot hr^{-1} \cdot m^{-2} \cdot bar^{-1}$ at the polymerization time of 75 s. PWP dropped drastically as much as 35% from 10 to 15 s but slowed down between 15 and 75 s. The reduction of PWP was an indication of the crosslinking and film growth effect, since PWP was a function of membrane material, thickness, and pore size. Figure 2 showed that at the very initial period of 5 s difference in polymerization time (10 to 15 s), the $\Delta x/A_k$ value was increased about 50%. The increase in skin thickness exerts the resistance for water transportation but the film growth became slower at longer polymerization times and no drastic increase of effective thickness could be observed. Besides that, the increase in crosslinking reduced the membrane porosity, which resulted in the increase of $\Delta x/A_k$.

However, the PWP value was observed to follow the reverse trend for higher polymerization time. PWP was increased as much as 13% from 4.94 $L \cdot hr^{-1} \cdot m^{-2} \cdot bar^{-1}$ at 75 s polymerization time to 5.58 $L \cdot hr^{-1} \cdot m^{-2} \cdot bar^{-1}$ at 120 s polymerization time. The result was expected because the pore size was increased from 0.49 to 0.68 nm following the reaction time from 75 to 120 s as shown in Figure 1. The increased pore size produced a more porous and permeable membrane that allowed higher water output.

While the network structure formed by the crosslinking reaction increases salt rejection at the expense of reducing flux, the carboxylic acid structure formed by the hydrolysis reaction increases water flux due to its hydrophilic properties.[9] Nevertheless, at higher polymerization times, more BA will be incorporated to produce a loose structure that is high in PWP.

Effect of polymerization time on NaCl rejection and flux

The NaCl rejection and flux profile was shown in Figure 7. The rejection ability was decreased initially about 32% from 10 s polymerization time to 45 s polymerization time but increased thereafter as much as 15% from 45 s polymerization time to 60 s polymerization time. This phenomenon could be explained by looking at the pore size as well as the charge density changes. Figure 1 showed that the pore sizes between 15 and 75 s polymerization time were varied only around 0.48 ± 0.01 nm, which means that the rejection profile is unlikely due to the steric hindrance effect. The increase of NaCl rejection from 30 to 120 s was likely caused by the increase of charge density as well as the increase of $\Delta x/A_k$. Szmczyk et al. carried out a simulation on the rejection ability under the effect of $\Delta x/A_k$ at pore radius = 0.5 nm; $D_+ = D_- = 10^{-9}$ $m^2 s^{-1}$; $J_v = 50$ $\mu m s^{-1}$, and normalized charge density of 1. It was also found that the solute retention increased with the increased of $\Delta x/A_k$ until the value of

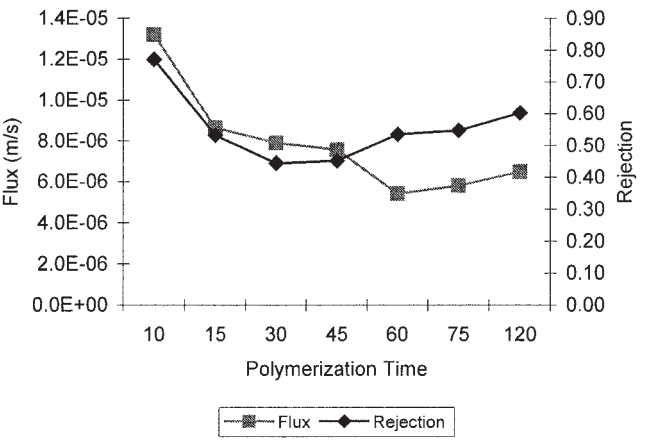

Figure 7 Comparison of flux and rejection of 0.01*M* NaCl at different polymerization times and 450 kPa operating pressure.

$\Delta x/A_k$ reached 5×10^{-6} m/s where it leveled off.[23] The maximum $\Delta x/A_k$ observed in this experiment below 75 s was 4×10^{-6} m/s and the $\Delta x/A_k$ value was found to be increasing linearly with the polymerization time. Therefore, it was possible that the increasing retention noted between 30 and 120s was a result of increasing $\Delta x/A_k$.

Szmczyk et al.[23] also carried out another simulation on the retention of 1–1 electrolyte at different normalized charge density (ξ) under the conditions of $r_p = 0.5$ nm, $\Delta x/A_k = 7$ μm; $D_+ = D_- = 10^{-9}$ $m^2 s^{-1}$, and $J_v = 1 \times 10^{-6}$ m/s. It was found that the retention was doubled (58 to 95%) when the normalized charged density increased from 1 to 10. This simulation showed that the effect of charge density on NaCl rejection played an important role in electrolyte rejection. Figure 7 also showed that the best rejection occurred for membranes that were polymerized at 10 and 120 s, respectively, because these membranes have relatively higher charge density, as shown in Figure 5. A drastic drop in the rejection ability from 10 to 15 s was observed because of the reduced charge density.

On the other hand, Figure 7 shows that the flux trends of NaCl were similar to the pure water permeability profile discussed in the preceding section. As polymerization time increased from 10 to 45 s, the value of flux dropped as much as 59% from 13.2 $\mu m s^{-1}$ at a polymerization time of 10 s to 5.42 $\mu m s^{-1}$ at a polymerization time of 60 s. The reduction in flux was again an indication for the crosslinking and film growth effect. The reverse trend of flux which is increased from 5.42 $\mu m s^{-1}$ (polymerization time of 60 s) to 6.49 $\mu m s^{-1}$ (polymerization time of 120 s) is also a typical phenomenon of growing pore size because of BA content.

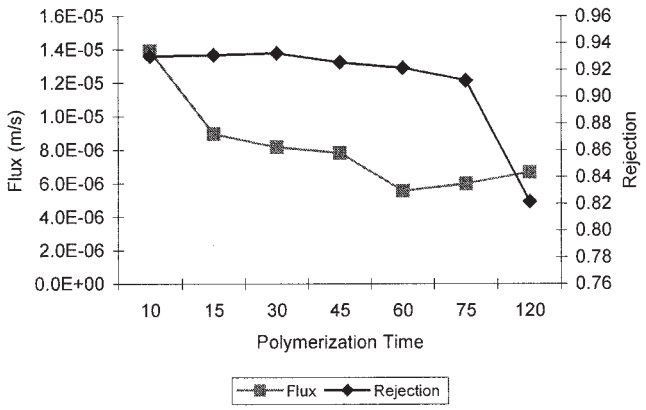

Figure 8 Comparison of flux and rejection of 300 ppm glucose at different polymerization times and 450 kPa operating pressure.

Effect of polymerization time on glucose rejection and flux

Figure 8 shows that the rejection profile of glucose was straightforward compared to the rejection profile of NaCl. A slight drop in rejection was observed for the glucose solution between 10 and 75 s polymerization time, while a sudden drop in rejection (10%) occurred at 120 s. The reduction in rejection was a result of growing pore size. Compared to the charged NaCl solute, glucose rejection is not affected by the introduction of the BA polar carboxylic group.

It was found that the flux profile of the glucose solution under the effect of polymerization time is similar to that of pure water and NaCl solution. For uncharged solute, the transport mechanism of glucose through the membrane was governed only by steric hindrance factor. However, with a r_s/r_p of approximately 0.80, the most likely transport process would be diffusion control. The $\Delta x/A_k$ parameter and charge density does not seem to be giving any effect to the retention ability of uncharged solute at limiting rejection.

CONCLUSION

Membrane skin layer properties strongly depend on polymerization time. For polypiperazinamide based membranes with the polymerization time between 10 and 75 s, the pore size was quite similar ($\sim$ 0.5 nm) and became larger at higher polymerization times. However, there was a proportional increase of effective membrane thickness/porosity when the reaction time increased after 10 s. Initially, surface charge was reduced drastically due to the film growth process and increased at longer reaction times due to the competing hydrolysis process as well as the incorporation of 3,5-diaminobenzoic acid. Effective membrane charge density for all the membranes depended on the degree of condensation and hydrolysis process. Polymerization times could change the effective thickness/porosity, pore size, and effective volume charge density and subsequently affect the membrane performance in terms of flux and rejection.

NOMENCLATURE

A_k: Porosity of the membrane

r_p: effective pore radius (m)

r_s: stokes radius of solutes or ions (m)

R_{real}: real rejection

Δx: effective membrane thickness (m)

X: effective membrane volume charge (mol m^{-3})

The authors are grateful to the financial support provided by Ministry of Science and Technology Malaysia through its Fundamental Research and IRPA grants.

References

1. Bruggen, B. V. D.; Everaert, K.; Wilms, D.; Vandecasteele, C. J Membr Sci 2001, 193, 239.
2. Vrijenhoek, E. M.; Waypa, J. J. Desalination 2000, 130, 265.
3. Volchek, K.; Velicogna, D.; Obenauf, A.; Somers, A.; Wong, B.; Tremblay, A. Y. Desalination 2002, 147, 123.
4. Akbari, A.; Remigy, J. C.; Aptel, P. Chem Eng Proc 2002, 41, 601.
5. Zhang, W.; He, G.; Gao, P.; Chen, G. Sep Pur Technol 2003, 30, 27.
6. Nguyen, M.; Reynolds, N.; Vigneswaran, S. J Cleaner Prod 2003, 11 803.
7. Paugam, L.; Taha, S.; Cabon, J.; Dorange, G. Desalination 2002, 152, 271.
8. Jayarani, M. M.; Kulkarni, S. S. Desalination 2000, 130, 17.
9. Rao, A. P.; Joshi, S. V.; Trivedi, J. J.; Devmurari, C. V.; Shah, V. J. J Membr Sci 2003, 211, 13.
10. Lu, X. F.; Bian, X. K.; Shi, L. Q. J Membr Sci 2002, 210, 1.
11. Mohammad, A. W.; Ali, N. Desalination 2002, 147, 205.
12. Labbez, C.; Fievet, P.; Szymczyk, A.; Vidonne, A.; Foissy, A.; Pagetti, J. J Membr Sci 2002, 208, 315.
13. Chen, S. H.; Chang, D. J.; Liou, R. M.; Hsu, C. S.; Lin, S. S. J Appl Polym Sci 2002, 83, 1112.
14. Kim, C. K.; Kim, J. H.; Roh, I. J.; Kim, J. J. J Membr Sci 2000, 165, 189.
15. Bowen, W. R.; Mohammad, A. W.; Hilal, N. J Membr Sci 1997, 126, 91.
16. Mohammad, A. W.; Ali, N.; Hilal, N. Sep Sci Technol 2003, 38, 1307.
17. Dubois, M.; Gilles, K. A.; Hamilton, J. K.; Rebers, P. A.; Smith, F. Anal Chem 1956, 28, 350.
18. Ahmad, A. L.; Ooi, B. S.; Choudhury, J. P. Desalination 2003, 158, 101.
19. Krantz, W. B.; Chai, G. Y. J Membr Sci 1994, 93, 175.
20. Labbez, C.; Fievet, P.; Szymczyk, A.; Vidonne, A.; Foissy, A.; Pagetti, J. Sep Pur Technol 2003, 30, 47.
21. Schaep, J.; Vandecasteele, C. J Membr Sci 2001, 188, 129.
22. Elimelech, M.; Zhu, X.; Childress, A. E.; Hong, S. J Membr Sci 1997, 127, 101.
23. Szymczyk, A.; Labbez, C.; Fievet, P.; Vidonne, A.; Foissy, A.; Pagetti, J. Adv Colloid Interface Sci 2003, 103, 77.